Journal of Physiology (1989), **418**, 427–439
With 8 text-figures
Printed in Great Britain

TRANSIENT AND PERSISTENT SODIUM CURRENTS IN NORMAL AND DENERVATED MAMMALIAN SKELETAL MUSCLE

BY PETER W. GAGE, GRAHAM D. LAMB* AND BRUCE T. WAKEFIELD

From the Department of Physiology, John Curtin School of Medical Research, Australian National University, Canberra, ACT, Australia

(*Received 30 March 1989*)

SUMMARY

1. Transient and persistent tetrodotoxin-sensitive sodium currents were recorded in response to depolarizing voltage pulses in voltage clamped segments of rat extensor digitorum longus muscle fibres at 20–25 °C in a triple Vaseline gap.

2. Appreciable persistent sodium current but little or no transient current was seen in response to depolarizations of up to 15 mV from a holding potential of −100 mV.

3. The maximum amplitude of both transient and persistent sodium currents occurred with depolarizations to −40 mV: the average peak amplitude of the transient current in fibres with a holding potential of −90 mV was $-0{\cdot}22 \pm 0{\cdot}03$ mA/μF (mean ± 1 S.E.M., seven fibres) and the average amplitude of the persistent current was $-0{\cdot}94 \pm 0{\cdot}10$ μA/μF (mean ± 1 S.E.M., twelve fibres). With a holding potential of −100 mV, the average amplitudes of the transient and persistent currents were $-0{\cdot}46 \pm 0{\cdot}10$ mA/μF (four fibres) and $-1{\cdot}4 \pm 0{\cdot}22$ μA/μF (five fibres), respectively.

4. The average maximum persistent sodium conductance in seven fibres held at −90 mV was $0{\cdot}13 \pm 0{\cdot}0078$ μS and the potential for half-maximum conductance was $-53 \pm 0{\cdot}74$ mV (mean ± 1 S.E.M.).

5. When the transient sodium current was completely inactivated with 100 ms conditioning depolarizations to potentials more positive than −50 to −60 mV, there was little inactivation of the persistent current.

6. In six denervated fibres, the average amplitudes of the transient and persistent sodium currents generated by pulses to −40 mV from a holding potential of −90 mV were $-0{\cdot}11 \pm 0{\cdot}01$ mA/μF and $-0{\cdot}88 \pm 0{\cdot}12$ μA/μF, respectively (mean ± 1 S.E.M.). It was concluded that there was a decrease in transient current but not persistent current amplitude following denervation and that the persistent current in denervated fibres with an increased input resistance could give rise to the spontaneous action potentials responsible for fibrillation.

INTRODUCTION

Spontaneous contractions commonly occur in denervated mammalian skeletal muscle, a phenomenon known as fibrillation. Both the contractions and underlying

* Present address: Department of Zoology, LaTrobe University, Bundorra, Victoria 3083, Australia.

MS 7607

spontaneous oscillations of membrane potential that produce repetitive action potentials can be blocked with extracellular solutions containing tetrodotoxin (TTX) or a low sodium concentration (Purves & Sakmann, 1974) suggesting that they are caused by a persistent (non- or slowly inactivating), TTX-sensitive sodium current.

Although persistent TTX-sensitive sodium currents have not previously been described in skeletal muscle, late and repeated openings of sodium channels have been seen in cultured skeletal muscle and cardiac muscle (Patlak & Ortiz, 1985, 1986). Furthermore, in other excitable membranes such as squid axon (Gilly & Armstrong, 1984) and mammalian hippocampal neurones (French & Gage, 1985), there is a persistent TTX-sensitive sodium current that activates at more negative potentials than the transient sodium current. It seemed possible that such a current might exist in skeletal muscle and be involved in the fibrillation seen in denervated muscle.

In order to explore this possibility, sodium currents were recorded in voltage-clamped normal and denervated mammalian muscle fibres using a technique that allowed effective blocking of other ionic currents.

METHODS

Membrane currents were recorded with the triple-Vaseline-gap clamp as described previously (Lamb, 1986). Adult male Wistar rats were killed by decapitation under halothane anaesthesia and the extensor digitorum longus (EDL) muscle was removed. A segment of a single fibre was dissected free and mounted in the Vaseline-gap chamber. The fibre was bathed internally with the following solution (mM): sodium glutamate, 135; Na-EGTA, 10; Mg-ATP, 3; Tris cyclic AMP, 1; Tris phosphocreatine, 5; TES buffer (*N*-tris(hydroxymethyl)-methyl-2-aminoethanesulphonic acid), 10; with the pH adjusted to 7·1 (with NaOH) and the osmolarity adjusted to 290 mosM. The external solution contained (mM): NaBr, 150; $CaBr_2$, 0·3; $MgBr_2$, 6; TES buffer, 2; 2,4-dichlorophenoxyacetic acid, 2·5 (to block chloride channels); sucrose, 40; with pH 7·3 and osmolarity 330 mosM. In most external solutions 10 μM-nifedipine (Sigma, USA) in ethanol was added to block the calcium channels. Tetrodotoxin (TTX; Sanko, Japan) was added from a 0·3 mM stock as required.

After 45 min exposure to the internal solution, the membrane potential of the fibre was clamped at -90 or -100 mV. The linear capacitance was determined by integrating the capacitive current generated by a 10 mV depolarizing step. In order to subtract most of the leakage and linear capacitive currents 'on-line', the command voltage was shaped and scaled so that it could be subtracted from and cancel the current generated by a 20 mV hyperpolarizing 'control' step that preceded each 'test' current. Any residual control current was later scaled and subtracted digitally from the accompanying test current. Most records were obtained by averaging four traces. Both voltage and current signals were filtered at 4 kHz by a 4-pole Bessel filter and sampled at 10 kHz by a DEC PDP11/23 microcomputer which also generated the voltage command sequence.

For experiments on denervated muscles, rats were anaesthetized with ether and a 1·5 mm segment of the sciatic nerve was removed in the region of the sciatic notch. The animals were then carefully monitored for 9–16 days before experimentation.

RESULTS

Transient and persistent sodium currents in normal fibres

Transient currents

Depolarization of a segment of muscle fibre in the Vaseline gap to potentials more positive than about -70 mV from holding potentials of -90 or -100 mV produced large transient inward currents. Typical currents generated by a voltage step from

−100 to −40 mV can be seen in Fig. 1 *A*. At potentials more negative than −40 mV, the transient current had two components, the slower of which was probably generated in the transverse tubular system as it was more prominent in fibres that had an obvious slower component of the capacity current; at potentials more

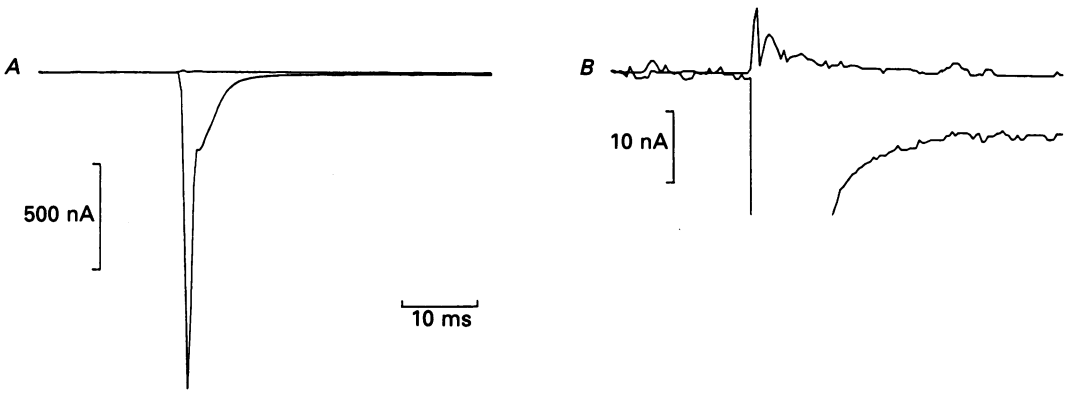

Fig. 1. Voltage steps to −40 mV from a holding potential of −100 mV generate transient and persistent sodium currents both of which are blocked by 1 μM-TTX. In *A*, traces recorded before and after exposure to TTX are superimposed. In *B*, the traces are shown at a higher gain to illustrate a persistent inward current in the control solution that disappears in the presence of TTX leaving an outward asymmetrical capacity current. Linear capacity and leakage currents have been subtracted using the currents generated by a voltage step from −100 to −120 mV.

positive than −40 mV, it merged with and could not be distinguished from the faster component. The amplitude at the peak of the transient current was near-maximal for pulses to −40 mV: the mean amplitude was $-1{\cdot}2 \pm 0{\cdot}15$ μA (mean ± 1 S.E.M.) in seven preparations with a holding potential of −90 mV. Normalizing this peak current to 'total capacity' (C_0), in order to take into account differences in membrane area between fibres, gave an average peak amplitude of $-0{\cdot}22 \pm 0{\cdot}03$ mA/μF (Table 1). The transient inward currents were completely blocked by TTX (1 μM) as can be seen by the trace close to the baseline in Fig. 1 *A*, confirming that they were sodium currents. The effect of TTX was readily reversible.

Persistent current

The transient currents were followed by a persistent inward current (Fig. 1*B*, lower trace). The persistent current was much smaller than the transient sodium current: in the records shown in Fig. 1, the peak transient current was $-1{\cdot}5$ μA whereas the amplitude of the persistent current at the end of the 50 ms pulse was −8·3 nA. In twelve preparations, the average amplitude of the persistent current at the end of a 50 or 100 ms pulse to −40 mV from a holding potential of −90 mV was $-5{\cdot}3 \pm 0{\cdot}53$ nA. The peak current normalized by the input capacity was $-0{\cdot}94 \pm 0{\cdot}10$ μA/μF. The average ratio of persistent to transient current amplitude in the seven preparations in which both were measured was $0{\cdot}49 \pm 0{\cdot}1$ %. The results for individual preparations can be seen in Table 1.

The persistent inward current was also blocked completely when a preparation was perfused with a solution containing 1 μM-TTX, as illustrated in the traces shown at

higher gain in Fig. 1*B*, indicating that it was also a sodium current. The residual transient outward current in the presence of TTX in Fig. 1*B* is a non-linear capacity current, often referred to as asymmetric charge movement.

Voltage dependence of the persistent current

The amplitude of the persistent current varied with potential as can be seen in Fig. 2. With a holding potential of −90 mV, a step to −70 mV produced a clear

TABLE 1. Normal fibres. Total resistance (R_0) and capacitance (C_0) were measured from the current generated by a 10 mV depolarizing pulse. The values for the peak of the transient current (I_t) and the persistent current (I_p) were obtained from currents generated by voltage steps to −40 mV. In some fibres, the transient currents saturated the amplifier and were not measured

		R_0 (MΩ)	C_0 (nF)	I_t (μA)	I_t (mA/μF)	I_p (nA)	I_p (μA/μF)	I_p/I_t (%)
				$V_h = -90$ mV				
Fibre no.	1	1·25	5·8	—	—	−9·2	−1·58	—
	2	2·24	8·3	—	—	−5·2	−0·63	—
	3	2·32	5·9	—	—	−5·5	−0·93	—
	4	2·50	6·5	—	—	−4·1	−0·63	—
	5	3·31	6·0	−0·97	−0·16	−4·6	−0·76	0·47
	6	2·12	5·1	—	—	−4·7	−0·92	—
	7	0·97	7·0	−1·33	−0·18	−3·2	−0·45	0·24
	8	2·73	7·2	−1·77	−0·24	−4·1	−0·57	0·23
	9	1·37	5·1	−1·71	−0·33	−4·1	−0·80	0·24
	10	3·19	6·8	−1·14	−0·16	−9·2	−1·34	0·80
	11	1·70	4·0	−0·51	−0·12	−5·0	−1·26	0·98
	12	1·90	3·6	−1·10	−0·30	−5·0	−1·38	0·46
Mean		2·1	5·9	−1·2	−0·22	−5·3	−0·94	0·49
S.E.M.		0·20	0·37	0·15	0·03	0·53	0·10	0·10
n		12	12	7	7	12	12	7
				$V_h = -100$ mV				
Fibre no.	11	1·70	4·0	−2·0	−0·51	−7·1	−1·79	0·35
	12	1·90	3·6	−2·7	−0·74	−7·7	−2·12	0·28
	13	3·51	5·7	−1·5	−0·26	−7·9	−1·38	0·52
	14	1·89	7·1	−2·1	−0·29	−4·9	−0·69	0·24
	15	1·05	4·3	—	—	−5·0	−1·16	—
Mean		2·0	4·9	−2·1	−0·46	−6·5	−1·4	0·35
S.E.M.		0·36	0·58	0·21	0·10	0·58	0·22	0·05
n		5	5	4	4	5	5	4

persistent inward current that became progressively larger with steps up to −40 mV and then became smaller at potentials more positive than −40 mV. The downward deflections at the end of the persistent currents, generated on return to the holding potential, are predominantly non-linear capacity currents as they were much the same size after exposure to TTX.

The amplitude of the persistent inward current, measured at the end of a 50 ms voltage step in another fibre, is shown plotted against potential in Fig. 3 (○). The current reversed at about −5 mV, close to the calculated sodium equilibrium potential of −0·5 mV. After exposure to TTX, the current completely disappeared (Fig. 3, ●). The amplitude of the persistent conductance calculated from the current

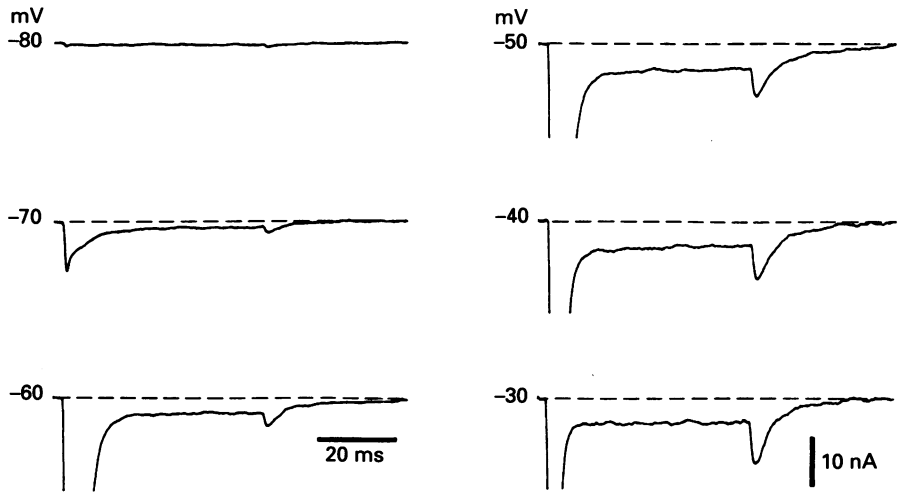

Fig. 2. Currents generated by voltage steps to the potentials indicated from a holding potential of −90 mV. Linear capacity and leakage currents have been subtracted using the currents generated by a voltage step from −90 to −110 mV. The larger transient currents have been truncated to show the persistent currents at higher gain. Horizontal calibration, 20 ms. Vertical calibration, 10 nA.

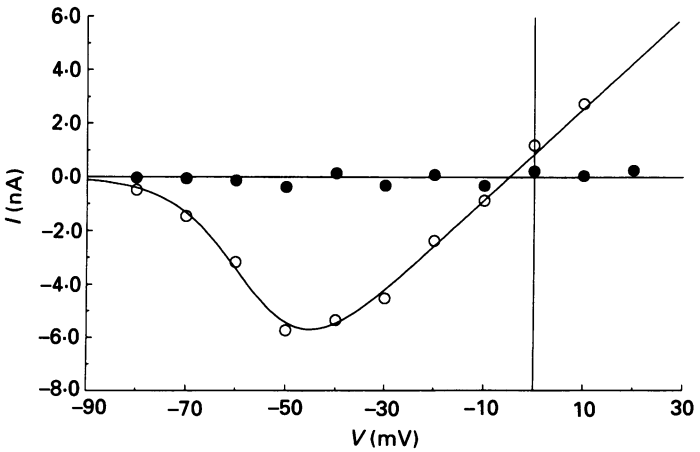

Fig. 3. The relationship between voltage and persistent current amplitude in control solution (○) and after exposure to TTX (●). The line through the open circles was calculated from the line in Fig. 4 using the relationship $I = g(V\text{-}E_{Na})$.

and the reversal potential is plotted against membrane potential in Fig. 4. The line through the points is the best fit of the Boltzman equation,

$$g = g_{max}/(1+\exp\{(V'-V)/k\}), \quad (1)$$

to the conductance values with $g_{max} = 0{\cdot}17\ \mu S$, $V' = -56$ mV and $k = 7$ mV (where

V' is the voltage for half-maximal conductance and k is a slope constant). Similar conductance–voltage curves were obtained in seven fibres: the average maximum conductance was $0{\cdot}13 \pm 0{\cdot}0078\ \mu S$, the half-maximum conductance occurred at $-53 \pm 0{\cdot}74$ mV and the average slope constant was $5{\cdot}6 \pm 0{\cdot}28$ mV (mean $\pm$ 1 S.E.M.).

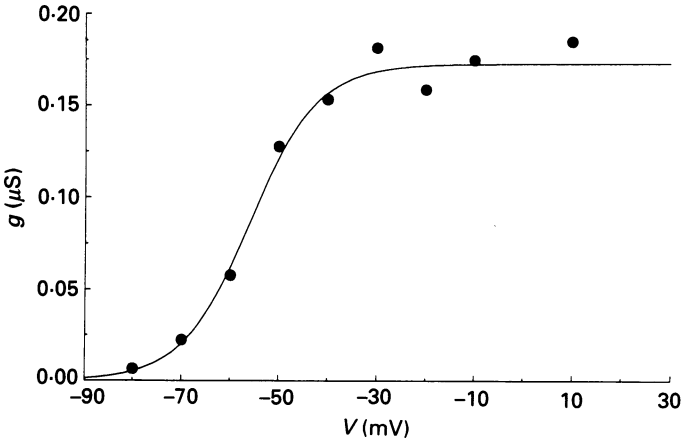

Fig. 4. Persistent sodium conductance (calculated from the data shown in Fig. 3) plotted against voltage. The line was drawn in accord with eqn (1) (see text).

Effect of holding potential

In several experiments in which a holding potential of -100 mV was used, both the transient and persistent currents were larger than with a holding potential of -90 mV but the effect on the transient currents was more pronounced. The average amplitude of the transient current in four preparations held at -100 mV was $-0{\cdot}46 \pm 0{\cdot}1$ mA/μF, about twice the average value for the seven fibres held at -90 mV. With a holding potential of -100 mV, the average persistent sodium current was $-1{\cdot}4 \pm 0{\cdot}22\ \mu$A/$\mu$F, about 50% larger than at -90 mV. In two fibres, sodium currents were recorded first with a holding potential of -90 mV (fibres 11 and 12, Table 1) and then -100 mV (fibres 11 and 12, Table 1). It can be seen that in both cases the transient current increased 2–3 times in amplitude while the persistent current increased by only 40–50%.

Differential inactivation of persistent and transient currents

A possible explanation for the persistent current is that a fraction of the channels that produce the transient current can recover from the inactivated state and repeatedly re-open in a depolarized membrane to produce the persistent current. If this were so, it might be expected that persistent currents should always be preceded by transient currents. However, it was often possible to record persistent, TTX-sensitive currents as potentials where there was little, if any, transient sodium current, as illustrated in Fig. 5. A voltage pulse to -90 mV from a holding potential of -100 mV elicited a small persistent inward current but no obvious transient current. With a voltage pulse to -85 mV there was a small transient inward current of much the same magnitude as the persistent current. At -80 mV, there was now

a prominent transient current with fast and slow components preceding the persistent current. Such observations indicate that the persistent current is not a constant fraction of the transient current but the ratio of the two varies with potential.

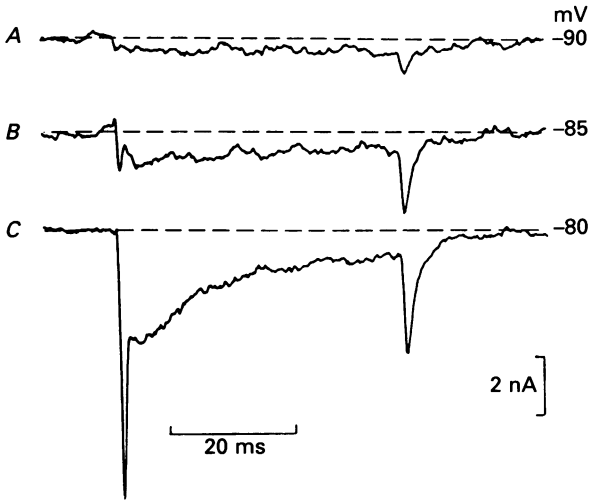

Fig. 5. Currents generated by small voltage steps from a holding potential of −100 mV. Note that at the most negative potentials there is a persistent current but no transient current. Linear capacity and leakage channels have been subtracted using the currents generated by a voltage step from −100 to −120 mV. Horizontal calibration, 20 ms. Vertical calibration, 2 nA..

In some records of the persistent current there appeared to be a steady decrease in the amplitude of the current during a 50 ms voltage pulse. This could have been due to inactivation of the persistent current or to the appearance of an outward current that was not completely blocked in the solutions used (see Methods). In order to explore the degree of inactivation of the persistent current, currents generated by a step to −20 mV were recorded following pre-pulses to different conditioning potentials. Results obtained in one of these experiments are illustrated in Fig. 6. Pre-pulses lasting 100 ms to potentials from −100 to −40 mV (from a holding potential of −90 mV) were used to compare the effects of a conditioning potential on transient and persistent currents produced by a test pulse to −20 mV. The pulse protocol is shown schematically in Fig. 6*A*. It can be seen from the records in Fig. 6*B* that the transient current following a conditioning pulse to −80 mV was about half the amplitude of the transient current following a conditioning pulse to −100 mV and that the conditioning pulses to −60 and −40 mV essentially completely inactivated the transient current. The relative lack of effect of these conditioning pulses on the persistent current can be seen in the traces shown at higher gain in Fig. 6*C*. The persistent inward currents generated by test pulses to −20 mV following conditioning pulses to −100 to −40 mV were little affected by the conditioning voltage pulses even when the transient current appeared completely inactivated after the conditioning pulse to −40 mV.

A graph of the amplitude of transient (△) and persistent currents (▲), relative to

their respective amplitudes following a conditioning pulse to −120 mV, are shown for a range of conditioning potentials in Fig. 7. The line through the points was drawn according to

$$I = I_{max}/(1+\exp\{(V-V')/k\}), \quad (2)$$

with V' and k values of −78 and 6 mV, respectively. The curves illustrate the

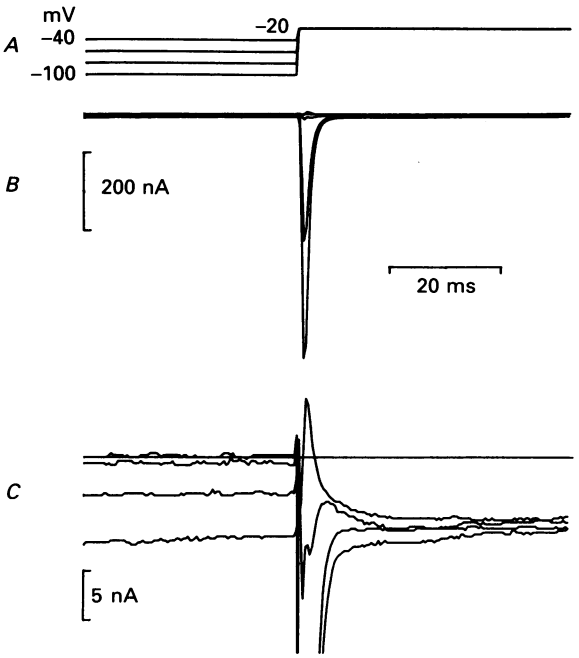

Fig. 6. Relative resistance of the persistent sodium current to inactivation. Currents were generated by a test pulse to −20 mV following 100 ms conditioning pulses to −100, −80, −60 and −40 mV. The pulse protocol is shown diagrammatically in *A*. Progressive inactivation of the transient sodium current as the pre-potential was made more positive is shown in *B*. Traces shown at higher gain in *C* show the relative lack of inactivation of the persistent sodium currents in the later sections of the traces.

observation that there was much less inactivation of the persistent current after 100 ms depolarization than of the transient current. The graph also shows that the relative amplitude of transient and persistent currents could be varied by changing the conditioning potential.

These observations suggested that, by suitable choice of conditioning pre-potential that completely inactivated the transient current, it should be possible to record the persistent current alone over a range of potentials. Persistent currents recorded in this way using a conditioning pre-pulse to −55 mV are illustrated in Fig. 8. Traces from *A* to *D* were generated by conditioning pulses to −55 mV followed by test pulses to −60 (*A*), −50 (*B*), −40 (*C*) and −30 mV (*D*). (The voltage pulse protocol used in this experiment is illustrated below the currents records.) It can be seen that the persistent current became progressively larger from −60 to −40 mV and became smaller at −30 mV, as seen when no conditioning pulse was used (see, for example,

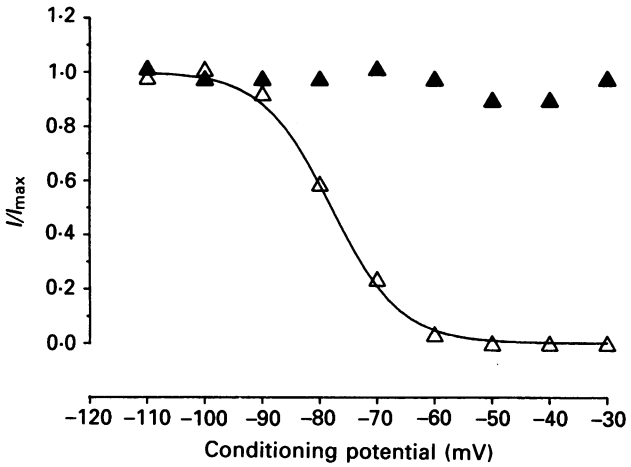

Fig. 7. Amplitude of the transient (△) and persistent (▲) sodium current, relative to the amplitude following a pre-potential of −120 mV, plotted against pre-potential amplitude. The line through the open triangles was drawn according to eqn (2) with V' and k values of −78 and 6 mV respectively.

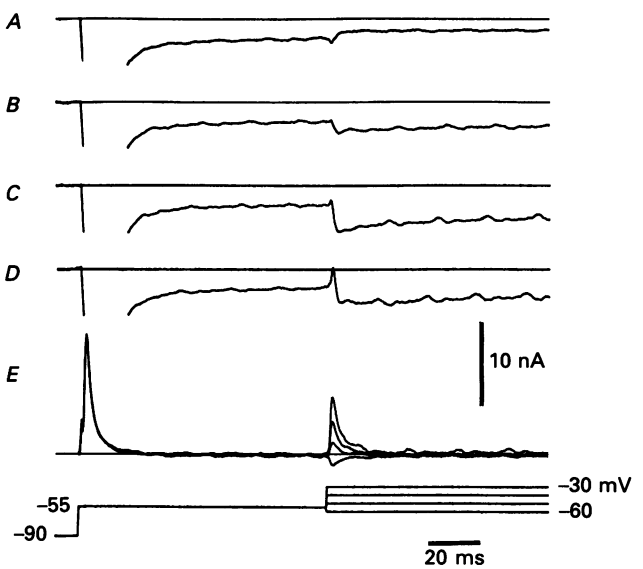

Fig. 8. Persistent sodium currents recorded by voltage steps to −60 (*A*), −50 (*B*), −40 (*C*) and −30 mV (*D*) following a conditioning pre-pulse to −55 mV used to inactivate the transient sodium current. The pulse protocol is shown diagrammatically below. The same pulse protocol produced no inward current after exposure to TTX (*E*).

Fig. 2). Currents generated in the same preparation after introduction of TTX (Fig. 8*E*) confirmed that the persistent sodium currents were not contaminated by other currents; the residual transient currents were capacity currents.

Transient and persistent sodium currents in denervated fibres

Transient and persistent currents were recorded in a total of seven fibres from muscles denervated for 10, 14 or 16 days. Both currents could be blocked reversibly

TABLE 2. Denervated fibres (symbols are as for Table 1)

		R_0 (MΩ)	C_0 (nF)	I_t (μA)	I_t (mA/μF)	I_p (nA)	I_p (μA/μF)	I_p/I_t (%)
				$V_h = -90$ mV				
Fibre no.	1	2·5	3·8	−0·48	−0·12	−2·3	−0·59	0·47
	2	1·5	2·8	−0·32	−0·11	−3·7	−1·32	1·14
	3	2·5	4·8	−0·69	−0·14	−4·0	−0·81	0·58
	4	5·8	3·3	−0·33	−0·09	−2·4	−0·71	0·73
	5	1·7	3·0	−0·21	−0·06	−3·7	−1·22	1·80
	6	3·0	2·7	−0·32	−0·11	−1·7	−0·63	0·53
Mean		2·8	3·4	−0·39	−0·11	−2·9	−0·88	0·88
S.E.M.		0·59	0·30	0·06	0·01	0·35	0·12	0·19
n		6	6	6	6	6	6	6
				$V_h = -100$ mV				
Fibre no.	5	1·7	3·0	−0·63	−0·20	−3·1	−1·02	0·49
	6	3·0	3·4	−0·83	−0·24	−3·1	−0·91	0·37
	7	5·12	2·8	−0·34	−0·12	−3·6	−1·27	1·06
Mean		3·3	3·1	−0·60	−0·19	−3·3	−1·1	0·64
S.E.M.		0·81	0·14	0·12	0·03	0·13	0·09	0·17
n		3	3	3	3	3	3	3

with TTX but a concentration of 10 μM rather than 1 μM was now necessary to eliminate the currents completely. The transient current was obviously smaller than in the normal fibres but the persistent current was not decreased to a similar degree.

Transient currents

With a holding potential of −90 mV, the average amplitude of the transient current was $-0{\cdot}39 \pm 0{\cdot}06$ μA, about a third of the average amplitude in the normal fibres (Table 2). Part of the decrease in current amplitude could have been due to a decrease in surface membrane area: the denervated fibres had a smaller diameter than normal which was reflected in a higher input resistance and lower total capacity than normal. However, even when the transient current was normalized to total capacity to take this difference into account (Table 2), the average amplitude in the denervated fibres was about half that in normal fibres. In three fibres in which records were obtained with a holding potential of −100 mV, the average amplitude of the transient current was −0·19 mA/μF compared with −0·11 mA/μF at −90 mV.

Persistent current

The persistent sodium current in the six denervated fibres was also smaller than in the normal fibres at the same holding potential (−90 mV) but the difference

disappeared when currents were normalized to total membrane capacity (Table 2). No significant difference was seen in the persistent current in three fibres with a holding potential of −100 mV.

The differential change in the transient and persistent currents is best seen by examining their relative sizes in the normal and chronically denervated preparations. In the six denervated fibres, the average ratio of the amplitudes of the persistent and transient currents was 0·88±0·19% (Table 2), significantly higher than the ratio of 0·49±0·010% in the seven normal fibres (Table 1).

Because of the very small amplitude of the persistent current in denervated fibres, it was not possible to measure current amplitude accurately over a range of potentials. For this reason the voltage dependence of the underlying conductance could not be determined.

DISCUSSION

The transient sodium current recorded in the normal fibres had a peak amplitude of −1·2±0·15 μA ($n = 7$) when the holding potential was −90 mV and −2·1±0·21 μA ($n = 4$) at a holding potential of −100 mV (means±1 S.E.M.). Taking membrane capacity into account, the average values become −0·22 and 0·46 mA/μF at the holding potentials of −90 and −100 mV, respectively (Table 1). If the slower component of the current is generated in the transverse (T−) tubular system and does not contribute significantly to the peak current, this figure would be an underestimate of the current density in the surface membrane. Using a figure of 6·5 μF/cm² for the capacity of the sum of the surface and T-tubule membrane in EDL fibres (Dulhunty, Gage & Lamb, 1986) and assuming a surface membrane capacity of 2 μF/cm² gives peak sodium conductances of 17·9 and 37·4 mS/cm² at the holding potentials of −90 and −100 mV, respectively. This is in reasonable agreement with the peak sodium conductance of 40–50 mS/cm² previously reported for 'detubulated' rat EDL muscle fibres held at −100 mV (Pappone, 1980).

In addition to the transient, rapidly inactivating sodium current, there is a small, persistent sodium current in these muscle fibres. Its presence has not been reported previously, probably because it is relatively small and can hardly be seen at gains used for the transient current; indeed, in many of our earlier experiments in which the amplifier gains were set to capture the persistent sodium current, the transient current could not be measured because it had saturated the amplifiers.

In terms of its size relative to the transient sodium current and its resistance to inactivation, the persistent sodium current described here is similar to the threshold sodium current in squid axons (Gilly & Armstrong, 1984) and the persistent sodium current in mammalian hippocampal neurones (French & Gage, 1985). In squid axon and hippocampal neurones, the persistent conductance–voltage curve rises at more negative potentials than the transient conductance–voltage curve so that a persistent sodium conductance is activated at potentials close to the resting membrane potential. Because it was assumed that membrane voltage was not controlled down the transverse tubular system during the transient current, it was not thought useful to compare the conductance–voltage relationship for the transient and persistent sodium currents in skeletal muscle but it was clear that the persistent current became

appreciably activated at potentials where there was little or no transient current, close to the resting membrane potential (Fig. 5). Indeed, the ratio of persistent and transient currents clearly decreased as the holding potential was made more positive (Tables 1 and 2).

The origin of the persistent sodium current is unclear. It may be that there is one homogeneous population of sodium channels with a high probability of complete inactivation but with a very low probability of opening late (either late first opening or reopening) during long depolarizations. Late opening sodium channels with the same conductance as early opening sodium channels have been seen in skeletal and cardiac muscle during long depolarizations (Patlak & Ortiz, 1985, 1986). The ratio of late opening to early opening channels was relatively constant from fibre to fibre and it was suggested that the late openings represented a mode of behaviour of a small fraction of the one population of sodium channels. The evidence available, however, does not exclude an alternative possibility that there is another kind of sodium channel responsible for the persistent current. This might explain the different voltage ranges over which the transient and persistent currents are activated and the wide variation in the relative amplitudes of the two types of current. It is interesting and perhaps relevant that the high molecular weight fraction of mRNA from rat or rabbit brain expresses sodium channels that inactivate very slowly in contrast to the sodium channels produced by unfractionated mRNA that inactivate rapidly (Krafte, Snutch, Leonard, Davidson & Lester, 1988). It may be that the assembly of subunits forming the channel responsible for the persistent sodium current is different from that responsible for the transient sodium current.

The decrease in amplitude of the transient sodium current per microfarad in denervated fibres may be related to the increase in membrane area in the transverse tubular system that occurs following denervation (Engel & Stonnington, 1974; Dulhunty & Gage, 1985). In other words, the transient current density in the surface membrane may be unchanged as reported in detubulated fibres (Pappone, 1980). The decrease in transient current per microfarad in denervated fibres with transverse tubular systems intact would explain the slower rate of rise of action potentials in denervated fibres (Albuquerque & Thesleff, 1968). On the other hand, the persistent sodium current per microfarad is not significantly changed following denervation. Because of the increase in input resistance that occurs in denervated fibres (Albuquerque & McIsaac, 1970) associated with a decrease in fibre diameter (Dulhunty & Gage, 1985), the same persistent sodium current in denervated fibres would be expected to cause a greater membrane depolarization than in normal fibres and could well produce the spontaneous action potentials responsible for fibrillation following denervation.

We thank Ann Andrews, Barbara McLachlan and Rod Malbon for their assistance and Drs Angela Dulhunty and Janet Nooney for comments on the manuscript. One of us (G.D.L.) was supported by a fellowship from the National Health and Medical Research Council.

REFERENCES

ALBUQUERQUE, E. X. & MCISAAC, R. J. (1970). Fast and slow mammalian muscles after denervation. *Experimental Neurology* **26**, 183–202.

ALBUQUERQUE, E. X. & THESLEFF, S. (1968). A comparative study of membrane properties of

innervated and chronically denervated fast and slow skeletal muscles of the rat. *Acta physiologica scandinavica* **73**, 471–480.

DULHUNTY, A. F. & GAGE, P. W. (1983). Asymmetrical charge movement in slow- and fast-twitch mammalian fibres in normal and paraplegic rats. *Journal of Physiology* **341**, 213–231.

DULHUNTY, A. F. & GAGE, P. W. (1985). Excitation–contraction coupling and charge movement in denervated rat extensor digitorum longus and soleus muscles. *Journal of Physiology* **385**, 75–89.

DULHUNTY, A. F., GAGE, P. W. & LAMB, G. D. (1986). Differential effects of thyroid hormone on t-tubules and terminal cisternae in rat muscles: an electrophysiological and morphometric analysis. *Journal of Muscle Research and Cell Motility* **7**, 225–236.

ENGEL, A. G. & STONNINGTON, H. H. (1974). Morphological effects of denervation of muscle. A quantitative ultrastructural study. *Annals of the New York Academy of Sciences* **228**, 68–88.

FRENCH, C. R. & GAGE, P. W. (1985). A threshold sodium current in pyramidal cells in rat hippocampus. *Neuroscience Letters* **56**, 289–293.

GILLY, WM. F. & ARMSTRONG, C. M. (1984). Threshold channels – a novel type of sodium channel in squid giant axon. *Nature* **309**, 448–450.

KRAFTE, D. S., SNUTCH, T. P., LEONARD, J. P., DAVIDSON, N. & LESTER, H. A. (1988). Evidence for the involvement of more than one mRNA species in controlling the inactivation process of rat and rabbit brain Na channels expressed in *Xenopus* oocytes. *Journal of Neuroscience* **8**, 2859–2868.

LAMB, G. D. (1986). Asymmetric charge movement in contracting muscle fibres in the rabbit. *Journal of Physiology* **376**, 63–83.

PAPPONE, P. A. (1980). Voltage-clamp experiments in normal and denervated mammalian skeletal muscle fibres. *Journal of Physiology* **306**, 377–410.

PATLAK, J. & ORTIZ, M. (1985). Slow currents through single sodium channels of the adult rat heart. *Journal of General Physiology* **86**, 89–104.

PATLAK, J. & ORTIZ, M. (1986). Two modes of gating late Na^+ channel currents in frog sartorius muscle. *Journal of General Physiology* **87**, 305–326.

PURVES, D. & SAKMANN, B. (1974). Membrane properties underlying spontaneous activity of denervated muscle fibres. *Journal of Physiology* **299**, 125–153.